Chapter 5

DFT And Statistical Mechanics

In the previous Chapter the combination of density-functional theory with concepts from thermodynamics has been discussed. Despite the very useful insight that can be obtained about the stability of different phases in a wide range of temperatures and pressures, this approach has two main limitations. First, the explicit time evolution of the system can not be treated and second, in the first-principles atomistic thermodynamics approach as it has been discussed here the sampling of the configurational space is rather limited.

In this Chapter the combination of DFT and statistical mechanics is described, which provides a more general concept to bridge the time and length scales between the electronic, meso- and macroscopic regimes as aspired by the multiscale modeling approach (cf. Fig. 4.1). *Equilibrium Monte Carlo* simulations can e.g. be used to identify again the thermodynamically most stable structure under different environmental conditions, but allows a wider sampling of configurational space. Using *kinetic Monte Carlo* simulations it is possible to explicitly treat the involved kinetics and therefore to also describe non-equilibrium situations. DFT will provide the basis to obtain the parameters needed as input to the simulations.

5.1 Monte Carlo Simulations

Computer simulations are a widespread tool to explicitly follow the trajectory of a system involving up to 10^4 degrees of freedom. A statistical analysis of the trajectory might then be used to predict properties of the simulated assembly of particles. Two general classes of simulations are *molecular dynamics* (MD) and *Monte Carlo* (MC) simulations.

In a molecular dynamics simulation atoms and molecules are viewed in a classical dynamical picture. Using forces extracted from the corresponding potential energy surface the trajectory can be formed by integrating Newton's equation of motion [85, 86]. If the forces are obtained from first-principles without any empirical or fitted parameters, the simulations are referred to as *ab initio* molecular dynamics.

A typical time scale that can be reached with such an *ab initio* molecular dynamics simulations [87] is of the order of picoseconds.

In a Monte Carlo method [86, 88], on the other hand, the configurational space is sampled in a stochastic manner to evaluate the partition function of the system. With such an *equilibrium* MC simulation one can obtain thermal averages of many particle systems, but the sequence of generated configurations does not reflect the real time evolution of the system. Thus the time connected to the simulation (so-called *MC time*) is not directly related to the *real time*.

In *kinetic* MC (kMC) simulations a proper relationship between MC time and real time is formed and a description of the dynamical evolution of the system becomes possible again. In contrast to a MD simulation only state-to-state transitions are treated rather than following the full microscopic trajectory. The resulting macroscopic trajectory, though, should be indistinguishable from the results of a MD simulation. As a consequence much larger time scales are accessible in a kMC simulation compared to a MD simulation.

Since in this work the simulations are used to investigate a system in a steady state of heterogenous catalysis, kinetic Monte Carlo is the most suitable choice. The rest of this Chapter will therefore be focussed on kMC.

5.1.1 Kinetic Monte Carlo

As already mentioned above a kinetic Monte Carlo step describes the transition from one system state into the next, while appropriately averaging over the whole microscopic motion of the atoms around their equilibrium position. The process of moving from one state to the next is also called a *rare event*, since on the time scale of atomic vibrations such a transition occurs only very seldom. Considering such a rare event it is assumed, that because the system stays relatively long in one state (compared to a vibrational period), there is no memory of how it got into this state. The probability to move from the present state S_i into the next state S_j is thus independent of whatever state preceded state S_i. The sequence of states generated for such a system is called a Markov chain, which as a result is a basic concept in Monte Carlo simulations. The probability for the transition from state S_i to state S_j, W_{ij}, can be expressed by the conditional probability, that the system is in state S_j at a time step t_n, if it has been in state S_i at the previous time step t_{n-1}

$$W_{ij} = W(S_i \to S_j) = P(X_{t_n} = S_j | X_{t_{n-1}} = S_i) \quad , \tag{5.1}$$

where X_t is the state of the system at time t. The total probability of the system being in a state S_j at a time t_n is then given by

$$\begin{aligned} P(X_{t_n} = S_j) &= P(X_{t_n} = S_j | X_{t_{n-1}} = S_i) P(X_{t_{n-1}} = S_i) \\ &= W_{ij} P(X_{t_{n-1}} = S_i) \quad . \end{aligned} \tag{5.2}$$

The time dependence of this probability is described by a *master equation* (transforming time from a discrete to a continuous variable and setting $P(X_{t_n} = S_j) = P(S_j, t)$)

$$\frac{dP(S_j,t)}{dt} = -\sum_i W_{ji} P(S_j,t) + \sum_i W_{ij} P(S_i,t) \quad . \tag{5.3}$$

A numerical solution of this master equation is provided by kinetic Monte Carlo simulations [89–93], i.e. with a kMC simulation it is possible to describe the time evolution of a system, that is characterized by Eq. (5.3). To ensure, that the system will attain thermal equilibrium the detailed balance criterion has to be fulfilled

$$W(S_j \to S_i) P_{\text{eq}}(S_j) = W(S_i \to S_j) P_{\text{eq}}(S_i) \quad , \tag{5.4}$$

where P_{eq} denotes the equilibrium probability. If a system is in thermal equilibrium and the detailed balance criterion is satisfied, then the average number of processes from state $S_j \to S_i$ will be the same as for the reverse process $S_i \to S_j$, i.e. every process is balanced to its reverse one. Thus the probability of any given system state will be constant and the system remains in equilibrium.

A classical example for a rare event is the diffusion of a particle from a lattice site st to a neighboring site st'. Here, the particle adsorbed on site st vibrates around its equilibrium position typically once every picosecond, whereas the diffusion of this particle to any neighboring site st' would happen on a time scale of microseconds. In a MD simulation the particle would correspondingly vibrate for roughly 10^9 time steps before a diffusion event would happen. If the diffusion event is the actually interesting part, it would just be computational unfeasible to do this in a MD simulation. In contrast, a kinetic Monte Carlo simulation would concentrate only on the diffusion event, the rare event in this example. Thus, the time scale reached in a kMC simulation is much larger than in a MD simulation and can be even in the order of seconds.

To practically perform a kMC simulation in a first step the investigated system is mapped onto a lattice. This is done to keep the number of included processes in a manageable range. There are also lattice free kMC simulations (cf. Section 5.3), which are computational much more demanding and will not be discussed here. In a second step a list of *all relevant* processes p on the lattice has to be set up and a rate has to be assigned to each process. The rate r_p then characterizes the probability to escape from the present system state by the process p. The simulation starts in some initial configuration of the system. A total rate R is defined as the sum over rates of all *possible* processes in the current configuration, $R = \sum_p r_p$. A certain process k is then randomly chosen by

$$\sum_{p=0}^{k-1} r_p \leq \rho_1 R \leq \sum_{p=0}^{k} r_p \quad , \tag{5.5}$$

with $\rho_1 \in]0,1[$ being a random number. The probability of selecting a process k is weighted by its rate r_k, i.e. a process with a large rate has a higher probability to be

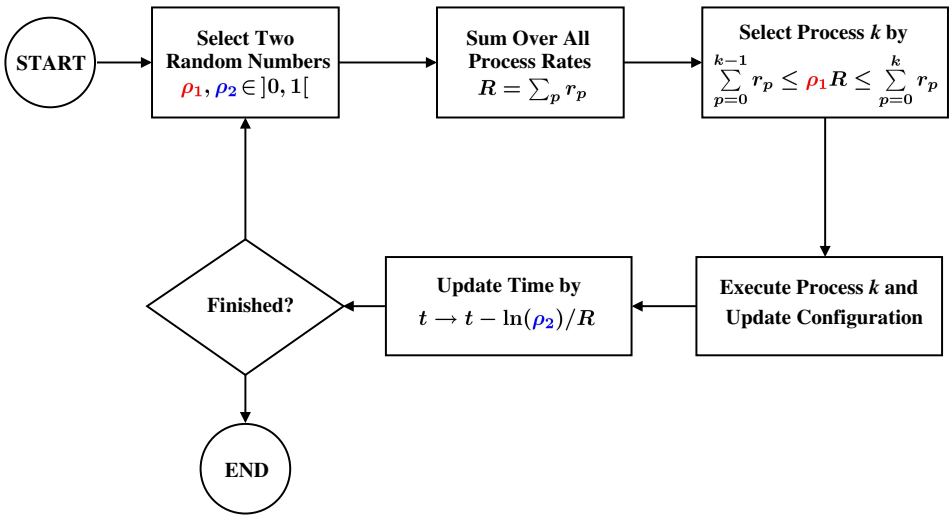

Figure 5.1: General flow chart for a kinetic Monte Carlo simulation. For each kinetic Monte Carlo step two random numbers are needed. Starting from some initial configuration the total rate is calculated as the sum over the rates of all possible processes. One process is selected by the first random number, it is then executed, the system configuration is updated and the time is advanced using the second random number.

chosen than a process with a very small rate. The selected process is executed and the configuration is updated. Since the kMC algorithm simulates a Poisson process, an explicit relationship between the MC time and the real time can be established [93]. After each kMC step the simulation time is updated according to

$$t \to t - \frac{\ln(\rho_2)}{R} \quad , \tag{5.6}$$

where $\rho_2 \in]0,1[$ is a second random number. For the new configuration again a new total rate R is determined, a process is selected and executed and the time is updated (cf. Fig. 5.1). Thus, the kMC simulation generates a sequence of system configurations on a realistic time scale.

Although the kMC algorithm is rather simple, there are several aspects, that have to be carefully considered. The identification of all possibly relevant processes and the determination of the corresponding process rates are crucial for the simulation. But the mapping onto a lattice and the identification of the relevant processes might not be obvious, which is one of the main problems in kMC simulations. If it is not desired or even possible to map the system onto a suitable lattice, so that a lattice free kMC simulation has to be performed, the setting up of a list of relevant processes and their corresponding rates is much more involved, still requiring further conceptional developments in this field. Additionally, such lattice free kMC simulations are computational very costly.

In the past the process rates were often obtained by fitting the results of the sim-

ulation to experimental data. Although this might lead to quite good results for the specific system, the rates have been fitted to, the transferability to other systems or other system conditions is highly questionable. An alternative way to calculate the process rates is given by using DFT or other electronic structure methods. If the rates are obtained without relying on experimental data, the method is referred to as *ab initio* kMC (for one of the first *ab initio* kMC simulations cf. Ref. [94]). The biggest advantage of a kMC simulation is, that for a system, where the considered rare events are well described by a Markov chain and where all possible processes and their rates are known, the kMC trajectory will be statistically indistinguishable from a MD trajectory, but on a much longer time scale.

5.1.2 Lattice Gas Hamiltonian

To calculate the process rates based on DFT it is necessary to evaluate the potential energy surface (PES) of the system in any possible configuration. Regarding the size of the simulated system and the number of possible configurations a direct calculation of the PES for each configuration with DFT is often computationally unfeasible.

If the investigated system can be mapped onto a lattice reflecting the different sites for the different species in the system, a lattice gas Hamiltonian (LGH) can be developed (analogous to an *Ising type model* [95] or a *cluster expansion* [96, 97]; the first *ab initio* LGH for surfaces has been published by Stampfl *et al.* [98]). Any system configuration can then be defined by the occupation of sites on the lattice, and the total energy can be expanded into a sum over the on-site energies F_i^0 (i.e. the energy of an isolated species on a lattice site i) and the interactions V between the different lattice sites .

$$H = \sum_i n_i F_i^0 + \sum_{ij} V_{ij} n_i n_j + \sum_{ijk} V_{ijk} n_i n_j n_k + \dots \tag{5.7}$$

The sums run over all lattice sites. V_{ij} is the interaction between two particles on lattice sites i and j (also called pair-interaction) and resp. V_{ijk} is the interaction parameter involving three particles on sites i, j and k (trio-interaction). The interaction parameters must be symmetric, i.e. $V_{ij} = V_{ji}$. n_l are the occupation numbers, i.e. $n_l = 0$ denotes, that site l is empty, and $n_l = 1$, that site l is occupied. If one could sum over all possible interactions, one should in principle obtain the correct energy. In practise the sum has to be truncated somewhere, which is a decisive task in constructing a LGH. Eq. (5.7) describes the lattice gas Hamiltonian for a system with only one particle species. Multiple sites are already included, but it should be noted that for an increasing number of site types, the number of non-equivalent interaction parameters increases rapidly. Also the description of a multicomponent, multisite system is straightforward by suitably expanding Eq. (5.7), with a resulting huge number of interaction parameters.

The on-site energies F_i^0 as well as the interaction parameters V contain a total energy as well as vibrational energy part. If the vibrational contribution of an adsorbate turns out to be rather independent of the surrounding atoms, the vibrational part of

the interaction parameter V can be neglected, which would be expected for the here discussed systems. To include the vibrational contribution in the on-site energies it is often sufficient to consider only the ZPE, since in the here discussed temperature range the vibrational contribution shows only a weak temperature dependence.

The evaluation of such a LGH is extremely fast, since just a simple sum has to be computed. The challenge in this approach is to determine the correct interaction parameters. Using DFT to calculate the parameters from first principles is the most reliable, but also the most demanding approach. A number of structures (at least as many as the number of interaction parameters) is calculated and the corresponding lattice gas Hamiltonian for every structure is set up, exploiting the periodic boundary conditions (i.e. also the interactions between the particle in the unit cell and its periodic images have to be considered). The obtained set of linear equations can be solved in several ways. If the number of equations is equal to the number of interactions, the interaction parameters can simply be calculated by direct inversion. If the number of calculated structures exceeds the number of interactions, the simplest approach would be a least square fit. Since the results obtained by direct inversion are usually not very accurate, the number of calculated structures should always be larger than the number of interaction parameters.

Another, more difficult task, is to decide, which interaction parameters have to be included in Eq. (5.7) and which can be set to zero. Since there is no automatized scheme for the truncation of the LGH, this is not obvious at all. Often the constructed LGH relies on intuition. One possibility to test the convergence of the LGH is its ability to predict the energy of computed configurations, that have not been included into the fitting procedure.

In this work the LGH approach has been used to determine the binding energies E^{bind} of different adsorbed species, that are needed to calculate the rates for the kinetic Monte Carlo simulation (cf. Section 5.2). Using Eq. (5.7) the binding energy of a particle on site i is given by

$$\begin{aligned} E_i^{\text{bind}} &= H(n_i = 1) - H(n_i = 0) \\ &= F_i^0 + 2\sum_j V_{ij} n_j + 3\sum_{jk} V_{ijk} n_j n_k + \dots \end{aligned} \tag{5.8}$$

By evaluating Eq. (5.8) any binding energy of a particle on any lattice site in any configuration can be obtained by a simple summation over the interaction parameters.

5.2 Determining The Process Rates

If the possible pathways for the transition from a state i to a state j are known, the rates for these processes needed in the kMC simulation can be calculated by transition state theory (TST). In this Section a derivation of the rates of the four main *types* of processes (adsorption, desorption, diffusion and reaction) included in the kMC

simulation of heterogeneous catalysis is presented (following the derivation given in Ref. [99]).

5.2.1 Transition State Theory

In the following discussion, transition state theory (TST) is only considered in its harmonic approximation, also often referred to as Vineyard theory [100]. In the harmonic TST the pathway connecting the initial and final state is characterized by a saddle point, the transition state (TS). The vibrational modes in the initial state and the vibrational modes perpendicular to the reaction coordinate at the transition state are assumed to be harmonic. The transition rate r^{TST} can then be expressed as [101]

$$r^{\mathrm{TST}} = \frac{\prod_{i=0}^{N} \nu_i^{\mathrm{init}}}{\prod_{i=0}^{N-1} \nu_i^{\mathrm{TS}}} \exp\left(-\frac{\Delta E^{\mathrm{TS}}}{k_{\mathrm{B}} T}\right) \quad , \tag{5.9}$$

where ν_i^{init} and ν_i^{TS} are the vibrational modes in the initial and transition state, respectively. N is the number of vibrational degrees of freedom and ΔE^{TS} is the energy difference between the transition state and the initial state. Since the harmonic approximation for the vibrational modes is used, which is valid for $h\nu \ll k_{\mathrm{B}} T$, the vibrational partition function for the initial $Z_{\mathrm{vib}}^{\mathrm{init}}$ and transition state $Z_{\mathrm{vib}}^{\mathrm{TS}}$ can simply be expressed by

$$Z_{\mathrm{vib}}^{\mathrm{init}} = \prod_{i=0}^{N} \frac{k_{\mathrm{B}} T}{h \nu_i^{\mathrm{init}}} \quad , \quad Z_{\mathrm{vib}}^{\mathrm{TS}} = \prod_{i=0}^{N-1} \frac{k_{\mathrm{B}} T}{h \nu_i^{\mathrm{TS}}} \quad . \tag{5.10}$$

Eq. (5.9) can then be reformulated to give an expression often seen in TST

$$r^{\mathrm{TST}} = \frac{k_{\mathrm{B}} T}{h} \frac{Z_{\mathrm{vib}}^{\mathrm{TS}}}{Z_{\mathrm{vib}}^{\mathrm{init}}} \exp\left(-\frac{\Delta E^{\mathrm{TS}}}{k_{\mathrm{B}} T}\right) \quad . \tag{5.11}$$

In addition to the prerequisite of having a saddle point another basic assumption in TST is that there is no recrossing of the TS, i.e. once the saddle point is reached the process will in any case follow the trajectory into the final state. However, if in reality recrossing of the TS takes place, the TST rate constant overestimates the exact rate, because some reactive events use up more than a single outgoing crossing. Although there are quite some approximations involved in deriving the process rates from TST, the obtained results are usually quite good at solid surface, where the potential energy surface is rather smooth. For such a simple system the dynamical bottleneck for transitions most often coincides with the saddle points on the PES. Especially for determining the rates of diffusion of ad-atoms on a surface this approximation has been proven very useful.

5.2.2 Adsorption

The rate of the adsorption of a gas molecule on a surface depends on the impingement rate and the sticking coefficient. The impingement rate can be calculated using kinetic gas theory, so that the rate of the adsorption of a gas phase species i on a surface site of type st can be written as

$$r_{i,st}^{\mathrm{ads}}(T, p_i) = \tilde{S}_{i,st}(T) \frac{p_i A}{\sqrt{2\pi m_i k_{\mathrm{B}} T}} \quad . \tag{5.12}$$

Here, A is the size of the surface unit cell and $\tilde{S}_{i,st}$ is the local sticking coefficient, which gives the fraction of impinging particles, that actually stick to the surface. Since the impinging gas phase particles have randomly distributed lateral positions as well as a random distribution over their internal degrees of freedom and Maxwell-Boltzmann distributed velocities, $\tilde{S}_{i,st}$ provides a statistical average over these degrees of freedom. The local sticking coefficient will become equal to the more commonly investigated initial sticking coefficient $S_{i,0}$ [87, 102], if there is only one site within the surface unit cell. For a kMC simulation, though, a specific rate of the adsorption for each site has to be considered, therefore $S_{i,0}$ can not be used for systems with more than one site type, since it does not contain site specific information.

To consider the influence of the lateral position of the impinging particles over the unit cell the concept of an *active area* inspired by the so-called hole model for adsorption [103] is applied. Here, it is assumed, that only particles of species i with an initial lateral position within a certain area $A_{i,st}$ around the adsorption site st of the total area A can actually stick to this site. The index i indicates that the active area can vary for different gas phase species. The local sticking coefficient will then be reduced by a factor

$$\frac{A_{i,st}}{A} \leq 1 \quad . \tag{5.13}$$

Inserting this expression into Eq. (5.12) it becomes obvious, that this factor effectively reduces the impingement rate. Only particles impinging within the active area $A_{i,st}$ can contribute to the site specific adsorption rate $r_{i,st}^{\mathrm{ads}}$. The adsorption rate is thus independent of the choice of a specific surface unit cell, but only depends on the active area for the respective site type and particle species. The sum over all active areas in a surface unit cell can not be larger than the unit cell area itself, i.e.

$$\sum_{st} A_{i,st} \leq A \quad , \tag{5.14}$$

because otherwise the number of considered sticking particles would exceed the original overall impingement rate.

In a classical picture an average over the internal degrees of freedom and the velocities would be described by the ability to overcome an energy barrier $\Delta E_{i,st}^{\mathrm{ads}}$ along the pathway to the surface. If all particles within the same active area would see the

same adsorption barrier, the local sticking coefficient would be given by

$$\tilde{S}_{i,st}(T) = \left(\frac{A_{i,st}}{A}\right) \exp\left(-\frac{\Delta E^{\mathrm{ads}}_{i,st}}{k_{\mathrm{B}}T}\right) \quad . \tag{5.15}$$

In the more general case of a high dimensional potential energy surface (PES) $\Delta E^{\mathrm{ads}}_{i,st}$ would correspond to the highest barrier along the minimum energy pathway (MEP), cf. Fig. 5.2. It can be expected, that on a more complicated PES not all the particles having a sufficiently high kinetic energy to overcome $\Delta E^{\mathrm{ads}}_{i,st}$ actually follow the MEP. Some of the particles will travel along pathways exhibiting higher energy barriers, at which they can be reflected. This will further decrease the sticking probability by a factor $f^{\mathrm{ads}}_{i,st} \leq 1$, so that Eq. (5.15) can be written in a more general form as

$$\tilde{S}_{i,st}(T) = f^{\mathrm{ads}}_{i,st}(T) \left(\frac{A_{i,st}}{A}\right) \exp\left(-\frac{\Delta E^{\mathrm{ads}}_{i,st}}{k_{\mathrm{B}}T}\right) \quad . \tag{5.16}$$

Whether a particle is steered along the MEP or not, depends on its initial state, i.e. the initial lateral position inside the surface unit cell A and the internal degrees of freedom. The calculation of $f^{\mathrm{ads}}_{i,st}$ would require dynamical simulations of trajectories of particles impinging on the surface. Since quite a number of such trajectories are needed to obtain a statistically meaningful average and each trajectory requires information about a large part of the PES [87], the computation of $f^{\mathrm{ads}}_{i,st}$ is rather demanding.

An alternative way to determine $f^{\mathrm{ads}}_{i,st}$ is TST. As explained in Section 5.2.1 the application of TST requires a saddle point, i.e. the adsorption process needs to be activated. Since $f^{\mathrm{ads}}_{i,st}$ quantifies the dependance of the sticking probability on the lateral position and internal degrees of freedom of the initial state, it can then be approximated by the ratio of all accessible states at the TS and in the initial gas phase state

$$f^{\mathrm{ads}}_{i,st} \approx f^{\mathrm{ads,TST}}_{i,st} = \frac{z^{\mathrm{vib}}_{i,st,\mathrm{TS}}}{z_{i,\mathrm{gas}}} \quad . \tag{5.17}$$

In the harmonic approximation all degrees of freedom in the TS are vibrational, so that only the vibrational partition function $z^{\mathrm{vib}}_{\mathrm{TS},i,st}$ is needed. To calculate the partition function at the TS and in the gas phase comparably less information about the PES are needed than for the dynamical simulations mentioned above. Nevertheless the identification of the TS is essential to this approach. Several methods have been developed to find the minimum energy pathway and in particular the corresponding saddle point. Depending on the complexity of the investigated PES identifying the TS can easily become the computational bottleneck in determining the rates. For an overview about transition state search algorithms see e.g. Ref. [104].

5.2.3 Desorption

Since the desorption process is the reverse process to the adsorption, the detailed balance criterion (Eq. (5.4)) has to be fulfilled. The probabilities for going from the

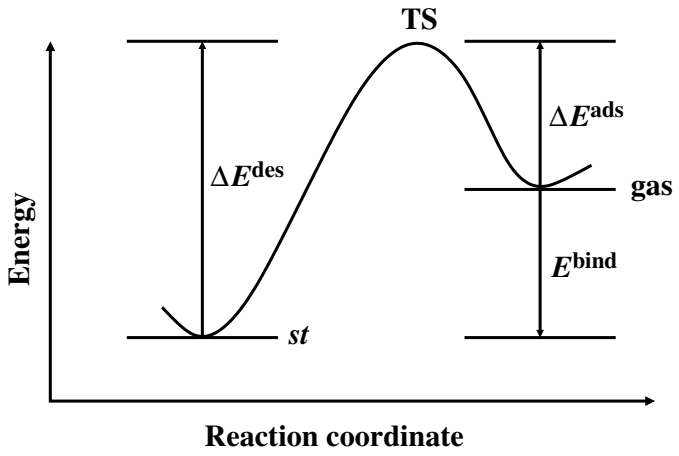

Figure 5.2: Schematic figure of a 1D reaction coordinate of a adsorption/desorption process. "*st*" refers to the adsorbed state of the particle on site *st*, "gas" to the gas phase state and "TS" to the transition state. If the transition state is clearly defined, the adsorption (ΔE^{ads}) and desorption barrier (ΔE^{des}) are determined as shown in the figure.

adsorbed into the desorbed state and vice versa ($W(S_{\mathrm{ads}} \to S_{\mathrm{des}})$ and $W(S_{\mathrm{des}} \to S_{\mathrm{ads}})$) are characterized by the desorption resp. adsorption rate. The ratio of the equilibrium occupation of the adsorbed and the desorbed state is given by the Boltzmann factor. The desorption and adsorption rates are then related by

$$\frac{r_{i,st}^{\mathrm{ads}}}{r_{i,st}^{\mathrm{des}}} = \exp\left(\frac{\Delta G_{i,st}(T,p_i)}{k_{\mathrm{B}}T}\right) \quad . \tag{5.18}$$

$\Delta G_{i,st}$ is the change in the Gibbs free energy between the particle in the gas phase and in the adsorbed state. If the pV term in the adsorbed state is neglected (i.e. $G \approx F$) the change in the Gibbs free energy can be expressed as

$$\Delta G_{i,st}(T,p_i) \approx \mu_{i,\mathrm{gas}}(T,p_i) - F_{i,st}(T) \quad , \tag{5.19}$$

where $\mu_{i,\mathrm{gas}}$ is the chemical potential of the gas phase and $F_{i,st}$ the free energy of the particle in the adsorbed state. The gas phase chemical potential can be further separated into a total energy part $E_{i,\mathrm{gas}}^{\mathrm{tot}}$ and a part $\Delta\mu_{i,\mathrm{gas}}$ (cf. Eq. (4.38)) containing the translational and internal (i.e. rotational and vibrational) degrees of freedom

$$\mu_{i,\mathrm{gas}}(T,p_i) = E_{i,\mathrm{gas}}^{\mathrm{tot}} + \Delta\mu_{i,\mathrm{gas}}(T,p_i) \quad . \tag{5.20}$$

The free energy of the particle in the adsorbed state can also be divided into a total energy part and a vibrational contribution

$$F_{i,st}(T) = E_{i,st}^{\mathrm{tot}} + F_{i,st}^{\mathrm{vib}}(T) = E_{i,st}^{\mathrm{tot}} - k_{\mathrm{B}}T\ln(z_{i,st}^{\mathrm{vib}}) \quad . \tag{5.21}$$

Combining Eq. (5.18) to (5.21) the ratio between adsorption and desorption rate can be rewritten as

$$\begin{aligned}\frac{r_{i,st}^{\mathrm{ads}}}{r_{i,st}^{\mathrm{des}}} =& \exp\left(\frac{(E_{i,\mathrm{gas}}^{\mathrm{tot}} + \Delta\mu_{i,\mathrm{gas}}(T,p_i)) - (E_{i,st}^{\mathrm{tot}} - k_{\mathrm{B}}T\ln(z_{i,st}^{\mathrm{vib}}))}{k_{\mathrm{B}}T}\right) \\ =& z_{i,st}^{\mathrm{vib}}\ \exp\left(\frac{\Delta\mu_{i,\mathrm{gas}}(T,p_i) - E_{i,st}^{\mathrm{bind}}}{k_{\mathrm{B}}T}\right) \quad ,\end{aligned} \tag{5.22}$$

where $E_{i,st}^{\mathrm{bind}}$ is the binding energy of a particle i at site st with respect to the gas phase as shown in Fig. 5.2, i.e. $E_{i,st}^{\mathrm{bind}} = E_{i,st}^{\mathrm{tot}} - E_{i,gas}^{\mathrm{tot}}$. Thus in addition to the adsorption rate only the binding energy $E_{i,st}^{\mathrm{bind}}$ as well as the vibrational partition function $z_{i,st}^{\mathrm{vib}}$ in the adsorbed state have to be known to calculate the desorption rate.

Also for the desorption rate an expression based on TST can be derived. Starting from Eq. (5.22) the explicit expression for the adsorption rate obtained from TST is inserted

$$\begin{aligned}r_{i,st}^{\mathrm{des}} =& r_{i,st}^{\mathrm{ads}}\ \frac{1}{z_{i,st}^{\mathrm{vib}}}\ \exp\left(-\frac{\Delta\mu_{i,\mathrm{gas}}(T,p_i) - E_{i,st}^{\mathrm{bind}}}{k_{\mathrm{B}}T}\right) \\ =& \frac{z_{i,st,\mathrm{TS}}^{\mathrm{vib}}}{z_{i,\mathrm{gas}}}\left(\frac{A_{i,st}}{A}\right)\exp\left(-\frac{\Delta E_{i,st}^{\mathrm{ads}}}{k_{\mathrm{B}}T}\right)\frac{p_i A}{\sqrt{2\pi m_i k_{\mathrm{B}}T}} \\ & \cdot\frac{1}{z_{i,st}^{\mathrm{vib}}}\exp\left(-\frac{\Delta\mu_{i,\mathrm{gas}}(T,p_i) - E_{i,st}^{\mathrm{bind}}}{k_{\mathrm{B}}T}\right)\end{aligned} \tag{5.23}$$

This expression can be much simplified by the following considerations. The partition function $z_{\mathrm{gas},i}$ for a particle in the initial state of an adsorption process (cf. Eq. (5.17)) can be divided into a translational part and the internal degrees of freedom, i.e.

$$z_{i,\mathrm{gas}} = z_{i,\mathrm{gas}}^{\mathrm{trans,2D}}\ z_{i,\mathrm{gas}}^{\mathrm{int}} = A\,\frac{2\pi m_i k_{\mathrm{B}}T}{h^2}\ z_{i,\mathrm{gas}}^{\mathrm{int}} \quad . \tag{5.24}$$

Also the translational and internal contribution to the chemical potential of the gas phase can be separated, giving

$$\Delta\mu_{i,\mathrm{gas}}(T,p_i) = -k_{\mathrm{B}}T\ln\left[\left(\frac{2\pi m_i k_{\mathrm{B}}T}{h^2}\right)^{3/2}\frac{k_{\mathrm{B}}T}{p_i}\right] - k_{\mathrm{B}}T\ln(z_{i,\mathrm{gas}}^{\mathrm{int}}) \tag{5.25}$$

Substituting $z_{i,\mathrm{gas}}$ and $\Delta\mu_{i,\mathrm{gas}}(T,p_i)$ in Eq. (5.23) by the expressions given in Eq. (5.24) and (5.25) will then yield the again rather simple expression for a desorption rate

$$r_{i,st}^{\mathrm{des}} = \left(\frac{A_{i,st}}{A}\right)\left(\frac{z_{i,st,\mathrm{TS}}^{\mathrm{vib}}}{z_{i,st}^{\mathrm{vib}}}\right)\left(\frac{k_{\mathrm{B}}T}{h}\right)\exp\left(-\frac{\Delta E_{i,st}^{\mathrm{des}}}{k_{\mathrm{B}}T}\right) \quad , \tag{5.26}$$

with

$$\Delta E^{\mathrm{des}}_{i,st} = \Delta E^{\mathrm{ads}}_{i,st} - E^{\mathrm{bind}}_{i,st} = E^{\mathrm{tot}}_{i,st\rightarrow \mathrm{gas,TS}} - E^{\mathrm{tot}}_{i,st} \tag{5.27}$$

being the desorption energy as shown in Fig 5.2. Thus for the calculation of the desorption rate based on TST again only knowledge of the transition state and the initial state, in this case the adsorbed state, is needed. By applying TST in the harmonic approximation the prefactor for the rate can be estimated without involving computationally demanding dynamical simulations. If the accuracy of this approximation is sufficient, depends on the investigated problem. Also, if there is no defined TS for a specific process, the application of harmonic TST is in any case invalid.

5.2.4 Diffusion

In a diffusion process the particle i moves from a site st to a site st'. If an appropriate saddle point along the diffusion pathway can be identified, analogous to the previous considerations harmonic TST can be applied to obtain the corresponding rate of diffusion. Similarly to Eq. (5.26) the diffusion rate is given by

$$r^{\mathrm{diff}}_{i,st\rightarrow st'}(T) = f^{\mathrm{diff,TST}}_{i,st\rightarrow st'}(T) \left(\frac{k_{\mathrm{B}}T}{h}\right) \exp\left(-\frac{\Delta E^{\mathrm{diff}}_{i,st\rightarrow st'}}{k_{\mathrm{B}}T}\right) \tag{5.28}$$

with

$$f^{\mathrm{diff,TST}}_{i,st\rightarrow st'}(T) = \frac{z^{\mathrm{vib}}_{i,st\rightarrow st',\mathrm{TS}}}{z^{\mathrm{vib}}_{i,st}} \tag{5.29}$$

and

$$\Delta E^{\mathrm{diff}}_{i,st\rightarrow st'} = E^{\mathrm{tot}}_{i,st\rightarrow st',\mathrm{TS}} - E^{\mathrm{tot}}_{i,st} \quad . \tag{5.30}$$

Just as the adsorption and desorption barriers (cf. Eq. (5.16) and (5.26)) the diffusion barrier denotes the maximum barrier along the minimum energy pathway of the diffusion process. The reverse process for the diffusion $st \rightarrow st'$ is simply the backward diffusion $st' \rightarrow st$. Thus, in determining the process rates for these two events the detailed balance criterion (Eq. (5.4)) must be considered to assure the attainment of thermal equilibrium.

5.2.5 Reaction

Following the above outlined derivation for the different rates, also a reaction process can be treated equivalently. If a reaction coordinate containing a saddle point can be established, the reaction rate can be determined using TST. The general form of the reaction rate is then given by

$$r^{\mathrm{reac}}_{i\rightarrow f}(T) = f^{\mathrm{reac,TST}}_{i\rightarrow f}(T) \left(\frac{k_{\mathrm{B}}T}{h}\right) \exp\left(-\frac{\Delta E^{\mathrm{reac}}_{i\rightarrow f}}{k_{\mathrm{B}}T}\right) \quad , \tag{5.31}$$

with now i denoting simply the initial state and f the final state of the reaction process. $\Delta E^{\mathrm{reac}}_{i\to f}$ is the reaction barrier determined by the difference in energy between the initial and the transition state

$$\Delta E^{\mathrm{reac}}_{i\to f} = E^{\mathrm{tot}}_{i\to f,\mathrm{TS}} - E^{\mathrm{tot}}_{i} \tag{5.32}$$

The prefactor $f^{\mathrm{reac,TST}}_{i\to f}$ can again be obtained from the ratio of the partition functions in the transition and initial state. With this, a rate of every possible reaction process can in principle be calculated. The most difficult task here is finding an appropriate reaction coordinate and transition state. If the rates are used in a kMC simulation it is also important to consider detailed balance (cf. Section 5.1.1). Thus the reverse reaction process has to be defined and an appropriate rate has to be taken into account.

In the kMC simulations presented in this work the considered reaction processes can in general be described by two particles A and B adsorbed on lattice sites st and st' reacting to form the product C, which then readily desorbs into the gas phase, i.e.

$$A_{st} + B_{st'} \to C_{\mathrm{gas}} \quad . \tag{5.33}$$

Such a reaction can equivalently be described as an associative desorption process, where the desorption barrier is given by the corresponding reaction barrier. The reverse process is then the dissociative adsorption of C onto the lattice sites st and st'. The adsorption barrier for this process is given by the sum of the reaction barrier and the binding energy of the reacting particles A and B on the surface (cf. Eq. (5.27)).

5.3 Summary

The combination of density functional theory and statistical mechanics provides a possibility to transfer information gained in the microscopic regime into the meso- and macroscopic one. Using kinetic Monte Carlo simulations the actual time evolution of the system can be followed over an extended time up to even seconds. This is achieved by only considering so called rare events, while appropriately coarse graining over the original microscopic motions of the system. The decisive parameters of a kMC simulation are then the lattice representing the system, the processes describing the evolution of the system and the corresponding process rates. A connection between kMC and DFT is established in the determination of the process rates. The rates can be derived using transition state theory and the for this needed information about the potential energy surface is provided by DFT.

The clear advantage of this approach is the independence of the simulation parameters from experimental results. Thus the results of the simulations can be analyzed on the basis of the included processes. By comparison with experimental data the quality of the kMC model (lattice and processes) can be checked and possibly improved. If the rates are not obtained from electronic structure calculations but by fitting to experimental results, the quality of the model is much more difficult to verify. Processes, which have been overlooked in the modeling, might be summarized in some

effective (unphysical) parameter with an effective rate obtained within the fitting procedure. Usually such fitted parameters exhibit a very small or no transferability to other systems or environmental conditions.

The most difficult and unsystematic part in a kMC simulation to date is the identification of relevant processes. Although some processes might be rather obvious, others might be overlooked or be completely unexpected. If a relevant process is missing from the beginning, of course also the results of a kMC simulation will miss the true physical behavior of the real system.

To overcome this limitation, some alternative approaches have been developed within recent years. One possibility is *on-the-fly kMC* [105], where the relevant processes are identified during the simulation by finding (all) possible pathways for the escape from the current state and the corresponding saddle points using the dimer-method [106]. Another possibility is *accelerated molecular dynamics* [107, 108]. Here, the classical trajectory is retained, but stimulated to find an appropriate escape pathway faster then a classical MD simulation. It should be noted though, that on the one hand such methods do not depend on the setup of a complete rate catalog, but on the other hand also here there is no guarantee for finding all possibly relevant processes. In addition these methods are usually computationally much more demanding. If a system is well described within a kMC approach as discussed in this Chapter, the kMC simulation provides a much more efficient way to follow the trajectory of a system over a mesoscopic time scale.